Time Dependent Composition in the December 2006 SEP Events

C.M.S. Cohen*, G.M. Mason†, R.A. Mewaldt*, E.E. Chollet*, E.R. Christian‡, A.C. Cummings*, M.I. Desai§, A.W. Labrador*, R.A. Leske*, E.C. Stone*, T.T. von Rosenvinge‡ and M.E. Wiedenbeck¶

**California Institute of Technology, Pasadena, California 91125*
†*Johns Hopkins Applied Physics Laboratory, Laurel, Maryland 20723*
‡*Goddard Space Flight Center, Greenbelt, Maryland 20771*
§*Southwest Research Institute, San Antonio, Texas 78228*
¶*Jet Propulsion Laboratory, California Institute of Technology, Pasadena, California, 91109*

***Abstract*. In large solar energetic particle (SEP) events the Fe/O abundance measured at a common energy/nucleon (E/M) often decreases with time. However, it has been found that for some events originating in the western solar hemisphere this time dependence lessens when Fe/O is calculated using O measured at a higher E/M than Fe. Such behavior may be the result of rigidity-dependent scattering processes in the interplanetary medium. We examine the time dependence of the Fe/O abundance in the December 2006 SEP events using ratios calculated at common and different E/M between 0.05 and 75 MeV/n and identify which O energy results in the least time-dependent Fe/O ratio for a given Fe energy. We compare time periods upstream and downstream of the shock arrivals and find the differences are more pronounced in the SEP event originating in the eastern solar hemisphere.**

***Keywords*: SEPs, Composition, Temporal Evolution**

I. Introduction

Abundance ratios in solar energetic particle (SEP) events are typically calculated at common energy/nucleon (E/M) values; however, studies throughout the past 30 years have shown that the temporal behavior of SEP intensities, such as time to maximum and decay constants, is rigidity dependent [1][2]. Thus, abundance ratios of elements with significantly different rigidities (e.g., O and Fe) are often time-dependent when calculated at the same E/M. A recent study of 14 western SEP events by Mason *et al.* [3] examined the temporal dependence of Fe/O when calculated at similar E/M values versus using O measured at a higher E/M. They found that, for many events, Fe/O showed significantly less time variation when O intensities at $(E/M)_O > (E/M)_{Fe}$ were used. The authors concluded that one possible explanation was interplanetary scattering, which would affect particles with the same diffusion coefficient similarly. The diffusion coefficient is related to the charge/mass ratio of the two ions examined; thus higher-E/M O would be affected similarly to lower-E/M Fe.

The Mason *et al.* [3] study examined western SEP events occurring between August 1997 and January 2005. Here we extend their work to two large SEP events (including one eastern event) observed in connection with two X-class flares on 6 and 13 December 2006. These were the last large SEP events of solar cycle 23; the first occurred when active region 10930 was near E63 solar longitude and the second when the region had rotated to W23. The spectral and compositional properties of these events are discussed in [4] and [5]. These events occurred shortly after the launch of the STEREO spacecraft when few instruments onboard were operational. The particle detectors on the Behind spacecraft observed both SEP events, while those on Ahead missed the second due to passing through the Earth's radiation belts. Both spacecraft were relatively near ACE and cross-calibration between instruments has revealed excellent agreement [4][5].

II. Data Analysis

The data used in this analysis are from the ULEIS [6] and SIS [7] instruments on ACE and the LET [8] instrument on STEREO Behind. The energy ranges covered by ULEIS, LET, and SIS for O are 0.05-8, 5-20, and 8-75 MeV/n respectively. Oxygen intensities from two energy channels from each sensor are shown in Fig. 1 as a function of time for the two SEP events. Two shocks were observed during the events and their passages are indicated by the solid vertical lines. Time periods were selected corresponding to upstream and downstream of the shock during each SEP event, yielding 4 separate periods: upstream_1, downstream_1, upstream_2, and downstream_2 (as indicated in Fig. 1).

We used three-hour averages for the O and Fe intensities and multiple Fe/O ratios were calculated as a function of time for each time period and each sensor. Mason *et al.* [3] concentrated on two Fe energies, 273 keV/n and 15 MeV/n; here we examine all the Fe energy channels available from each instrument, a total of 23 channels. For each Fe channel, Fe/O ratios were determined using all O intensities where $(E/M)_{Fe} \leq (E/M)_O \leq 5(E/M)_{Fe}$ within a given sensor. This is illustrated in the top left panel of Fig. 2 which shows the time dependence of the Fe/O ratios calculated using the 0.2 MeV/n Fe intensity and five O intensities measured at energies between 0.2 and 0.8 MeV/n during the 6

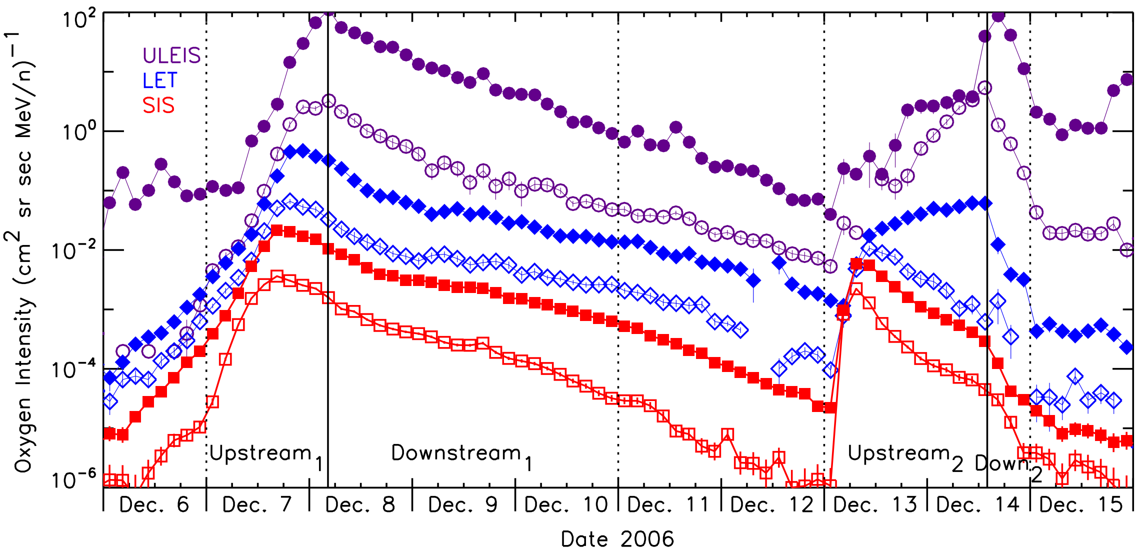

Fig. 1: Three-hour averaged O intensities from ULEIS (circles) at 0.14 (solid) and 1.5 (open) MeV/n, LET (diamonds) at 4.9 (solid) and 12 (open) MeV/n, and SIS (squares) at 18 (solid) and 34 (open) MeV/n. Solid lines mark shock passages and dashed lines mark boundaries of the selected upstream and downstream regions.

December event by ULEIS. Three other examples using different energy Fe intensities are also shown.

Plots like these for each value of $(E/M)_{Fe}$ measured by ULEIS, LET, and SIS were examined (by eye) for the four time periods to determine which value of $(E/M)_O$ resulted in the least time dependence. The corresponding value of $(E/M)_O/(E/M)_{Fe}$ was recorded; where there was no ratio that appeared flatter than the others, no $(E/M)_O/(E/M)_{Fe}$ was recorded. The resulting values are plotted as a function $(E/M)_{Fe}$ in Fig. 3. The panels show the two SEP events; the different symbols distinguish values determined for the upstream and downstream time periods. The analysis requires $1 \leq (E/M)_O/(E/M)_{Fe} \leq 5$ and the values are quantized by the channel spacing inherent to each instrument.

III. Discussion

As can be seen from Fig. 1 the shock arrived ∼1 day after the start of upstream$_1$ yielding an upstream time period significantly shorter than the downstream period for the 6 December event. The reverse is true for the 13 December event where the downstream$_2$ period was artificially truncated by the injection of additional H and He SEPs associated with an X-class flare late on 14 December [9]. During the upstream$_1$ period, none of the ULEIS Fe/O ratios with $(E/M)_{Fe} \leq 0.2$ MeV/n are flat (see, e.g., the top-left panel of Fig. 2), so no $(E/M)_O/(E/M)_{Fe}$ values are reported. In the downstream$_1$ portion it was also difficult to select $(E/M)_O/(E/M)_{Fe}$ values for $(E/M)_{Fe} \leq 0.2$ MeV/n as all ratios are relatively flat.

Unfortunately, there are no statistically significant LET Fe/O ratios available for downstream$_2$. During upstream$_1$ and upstream$_2$ the LET data show substantial differences in the temporal dependence of the ratios (bottom-left panel of Fig. 2), with the largest being in the second event. The ratios from SIS also show large variations in the upstream regions (Fig. 2, bottom-right panel). The passage of the shock did not have a noticeable affect on the SIS ratios in either event (Fig. 2, top-right panel).

The pattern seen in the bottom panels of Fig. 2 during upstream$_2$, where the Fe/O traces converge and then diverge again in a bowtie-like manner, is seen to a lesser degree for many other $(E/M)_{Fe}$ values in all three sensors. There is a hint of a similar pattern in the SIS data for upstream$_1$ but not for the other datasets. The most likely cause of this bowtie feature is the competition between velocity dispersion and diffusion. Ions of different velocities will exhibit different rise times, reaching maxima that are later for slower particles. The decay rate of the particle intensities is dependent on rigidity [2] with the intensities of higher rigidity particles decaying faster than those of lower rigidity. During the period contained in the left side of the bowtie feature (e.g., 13 Dec 00:00-04:00; lower-right panel), the higher-energy O intensities are strongly increasing while the Fe intensity is just starting to rise (Fig. 4), causing Fe/O to decrease. For O intensities at energies lower than that of Fe, the effect is reversed causing Fe/O to increase. After the crosspoint of the bowtie, the higher-energy O intensities have started to peak and decay before the Fe intensity has reached a maximum, causing Fe/O to increase (Fig. 4). Again, for O intensities at energies lower than that of Fe, the effect is reversed.

We have not reported uncertainties for the

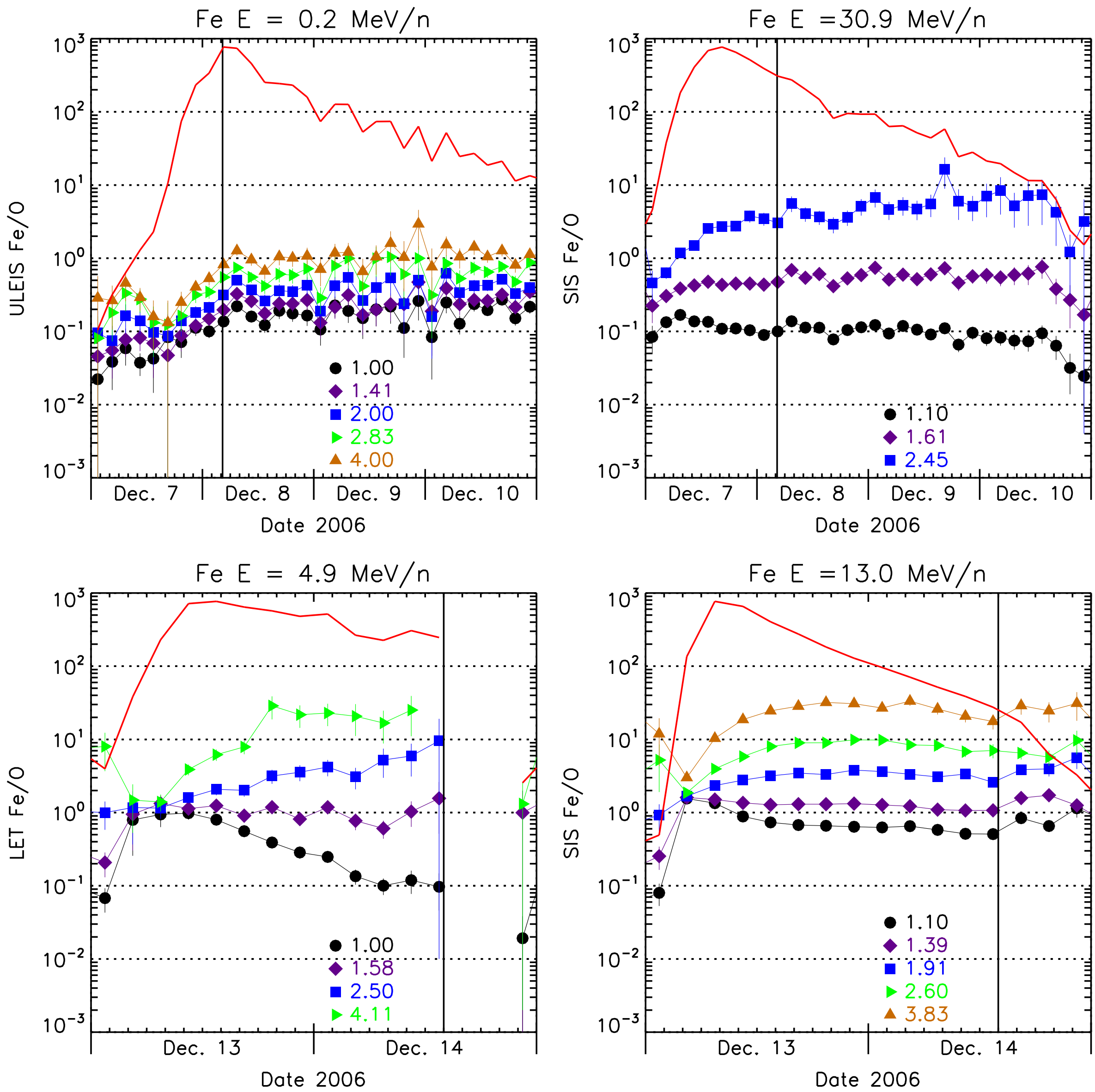

Fig. 2: Examples of temporal evolution of Fe/O calculated using O intensities for $(E/M)_O \geq (E/M)_{Fe}$ (values of $(E/M)_O/(E/M)_{Fe}$ are given in the legend) for 4 different $(E/M)_{Fe}$. The top (bottom) row shows examples from the first (second) SEP event. Solid lines indicate shock passages and upstream (downstream) intervals are to the left (right) of the shock. The Fe intensities (no symbols) are overlaid for reference (arbitrarily scaled).

$(E/M)_O/(E/M)_{Fe}$ values shown in Fig. 3 as they were determined by eye and are rather subjective. However, some trends can be seen. For the SEP event on 6 December, the values of $(E/M)_O/(E/M)_{Fe}$ that produced the least-time-dependent Fe/O are highest for energies below $\sim$1 MeV/n. The downstream$_1$ values appear to be roughly energy-independent at energies $\geq$ 4 MeV/n. At nearly all energies the downstream$_1$ values are generally higher than those determined for upstream$_1$. $(E/M)_O/(E/M)_{Fe}$ values near 1 were only found in the upstream$_1$ region at Fe energies above a few MeV/n.

The $(E/M)_O/(E/M)_{Fe}$ values in the 13 December SEP event show different tendencies than those in the previous SEP event; the values peak at energies near 1 MeV/n. Above a few MeV/n, values in upstream$_2$ and downstream$_2$ are comparable and roughly independent of energy (similar to downstream$_1$). There are almost no values near 1 in this event. It can be seen from the time profiles in Fig. 1 that the O intensities transition from peaking coincident with the shock passage to peaking prior to it at energies around 5-10 MeV/n. For higher energies, the shock arrival has little effect and thus the differentiation between ‘upstream’ and ‘downstream’ is artificial and reflected in the similarity of the obtained $(E/M)_O/(E/M)_{Fe}$ values. This is not the case in

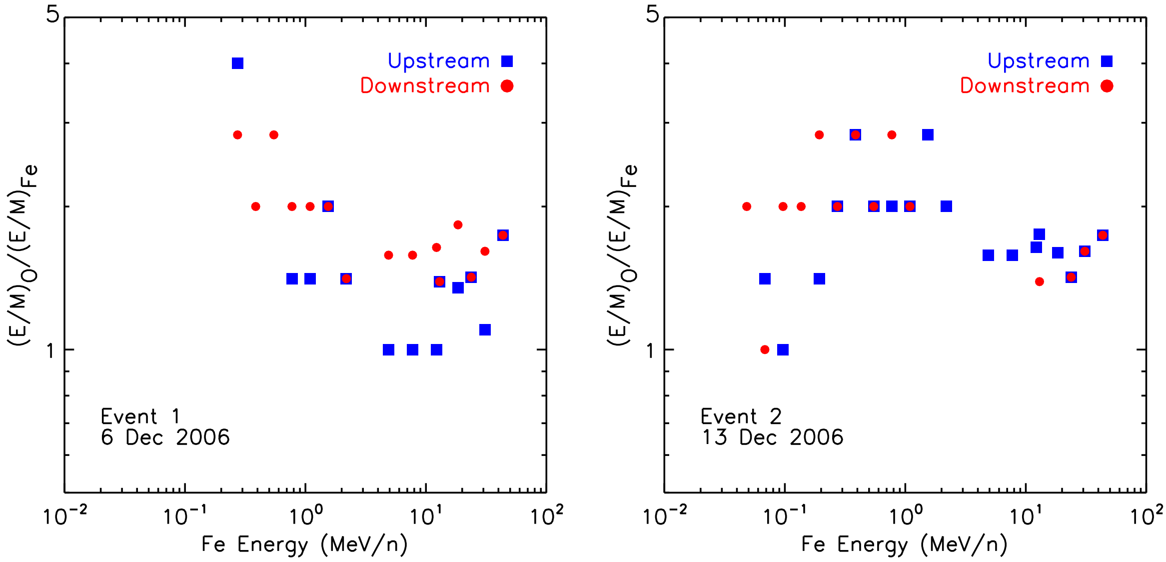

Fig. 3: Optimal values of $(E/M)_O/(E/M)_{Fe}$ versus $(E/M)_{Fe}$ for the two SEP events, upstream (blue squares) and downstream (red circles) of the shock passage.

the first SEP event, where nearly all the intensities peak close to the shock passage. Thus, even at high energies the upstream$_1$ period has little contribution from the decaying portion of the SEP event, which is reflected in the larger differences in the upstream$_1$ and downstream$_1$ $(E/M)_O/(E/M)_{Fe}$ values.
Mason *et al.* [3] obtained values for $(E/M)_O/(E/M)_{Fe}$ at 15 MeV/n for ten events, with six resulting in a value of 1.9. This is slightly higher than those obtained here at similar energies. At 273 keV/n, seven of Mason *et al.*'s values (out of 13) were 2.0 and three were 2.8, very similar to our results for the second (western) SEP event. Even at the lower energy, Mason *et al.* were able to select one $(E/M)_O/(E/M)_{Fe}$ value that reduced the time-dependence of Fe/O throughout the rise and decay of the events (see, e.g., Fig. 2 of [3]). Above ∼0.2 MeV/n we obtained similar values in the upstream$_2$ and downstream$_2$ periods, however this was not the case for Fe energies below that or for the 6 December SEP event, which originated in the east. It would be illuminating to perform our analysis of all ULEIS and SIS energy channels for the 14 events of Mason *et al.*, to see if the results presented here for the 13 December event are representative of other western SEP events. Of interest would be whether the 'peak' in $(E/M)_O/(E/M)_{Fe}$ values near 1 MeV/n is typical.

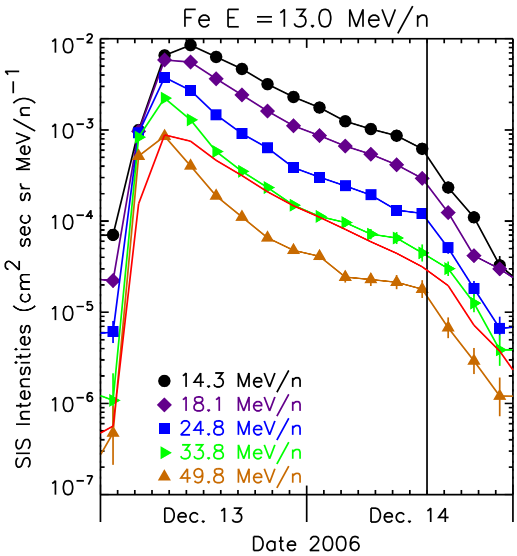

Fig. 4: Intensities of O (symbols) at the different energies used for the ratios in Fig. 2, lower-right panel. The Fe intensity is shown in red (no symbols).

Acknowledgements

This work was supported by NASA grants NAS5-03131, NNX08AI11G, and NAG5-6912 and NSF grant ATM04-54428.

References

[1] W.F. Dietrich & A.J. Tylka, *Proc. 27th ICRC (Hamburg), 27*, 3173, 2001.
[2] L.S. Sollitt, et al., *ApJ, 679*, 910, 2008.
[3] G.M. Mason, et al., *ApJ Letters, 647*, L65, 2006.
[4] C.M.S. Cohen, et al., *AIP Conf. Proc., 1039*, 118, 2008.
[5] R.A. Mewaldt, et al., *Proc. 30th ICRC (Merida), 1*, 107, 2008.
[6] G.M. Mason, et al., *Space Sci. Rev., 86*, 409, 1998.
[7] E.C. Stone, et al., *Space Sci. Rev., 86*, 357, 1998.
[8] R.A. Mewaldt, et al., *Space Sci. Rev.*, doi: 10.1007/s11214-007-9288-x, 2007.
[9] T.T. von Rosenvinge, et al., *Solar Phys., 256*, 443, 2009.